

# Analysis of Spherical, Rolling Magnet Generator for Passive Energy Harvesting

by

Cheng Gong

Department of Mechanical Engineering and Materials Science  
Duke University

Date: \_\_\_\_\_

Approved:

\_\_\_\_\_  
Brian Mann, Supervisor

\_\_\_\_\_  
Sophia Santillan

\_\_\_\_\_  
Michael Zavlanos

A thesis submitted in partial fulfillment of the  
requirements for the degree of Master of Science  
in the Department of Mechanical Engineering and Materials Science  
in the Graduate School of  
Duke University

2021

ABSTRACT

Analysis of Spherical, Rolling Magnet Generator for Passive  
Energy Harvesting

by

Cheng Gong

Department of Mechanical Engineering and Materials Science  
Duke University

Date: \_\_\_\_\_

Approved:

\_\_\_\_\_  
Brian Mann, Supervisor

\_\_\_\_\_  
Sophia Santillan

\_\_\_\_\_  
Michael Zavlanos

An abstract of a thesis submitted in partial fulfillment of the  
requirements for the degree of Master of Science  
in the Department of Mechanical Engineering and Materials Science  
in the Graduate School of  
Duke University

2021

Copyright © 2021 by Cheng Gong  
All rights reserved

# **Abstract**

In this thesis, a spherical, rolling magnet generator for passive energy harvesting is investigated. It was designed for gathering energy from human motion. This thesis focuses on the analysis of the dynamics of this device and gives its governing equations. Then under two expected applications, this thesis finds the parameters that greatly influence its efficiency and provide optimal parameter combinations.

# Contents

<b>Abstract</b>	<b>iv</b>
<b>List of Figures</b>	<b>vii</b>
<b>List of Tables</b>	<b>ix</b>
<b>Acknowledgements</b>	<b>x</b>
<b>1 Introduction</b>	<b>1</b>
<b>2 Equation of Motion Derivation</b>	<b>3</b>
2.1 Mechanical equations . . . . .	4
2.1.1 Lagrange equation in non-inertial system . . . . .	4
2.1.2 Motion of the sphere magnet . . . . .	5
2.2 Electrical equations . . . . .	6
2.2.1 Generalized Lagrange equation . . . . .	7
2.2.2 Magnet–coil interactions . . . . .	8
2.3 Governing equations . . . . .	12
2.3.1 Simplification of $f(\theta)$ . . . . .	13
<b>3 Numerical Simulation</b>	<b>15</b>
3.1 Horizontal harmonic excitation . . . . .	15
3.1.1 Different sphere magnet . . . . .	16
3.1.2 Different AWG . . . . .	18
3.1.3 Optimal parameter combination . . . . .	22
3.2 Vertical harmonic excitation . . . . .	23
3.2.1 Different sphere magnet . . . . .	24

3.2.2	Different AWG . . . . .	25
3.2.3	Optimal parameter combination . . . . .	27
<b>4</b>	<b>Conclusions</b>	<b>31</b>
4.1	Future work . . . . .	32
	<b>Bibliography</b>	<b>33</b>

# List of Figures

2.1	Schematic of sphere . . . . .	3
2.2	Electrical system circuit configuration diagram . . . . .	7
2.3	Schematic of magnet–coil interactions . . . . .	9
2.4	Dipole Direction . . . . .	10
2.5	Coil size . . . . .	11
2.6	Data points in the coil plane . . . . .	13
3.1	$f(\theta)$ under initial parameters . . . . .	17
3.2	Instantaneous power under initial parameters . . . . .	18
3.3	Instantaneous power of each sphere magnet . . . . .	19
3.4	Mean Power and RMS Voltage of each magnet . . . . .	20
3.5	Instantaneous power from AWG 29 to 32 . . . . .	21
3.6	Instantaneous power from AWG 33 to 36 . . . . .	22
3.7	Mean Power and RMS Voltage of each AWG . . . . .	23
3.8	Instantaneous power . . . . .	24
3.9	Instantaneous voltage . . . . .	25
3.10	Instantaneous power of each sphere magnet . . . . .	26
3.11	Mean Power and RMS Voltage of each magnet . . . . .	27
3.12	Instantaneous power from AWG 29 to 32 . . . . .	28
3.13	Instantaneous power from AWG 33 to 36 . . . . .	29

3.14 Mean Power and RMS Voltage of each AWG . . . . .	29
3.15 Instantaneous power . . . . .	30
3.16 Instantaneous voltage . . . . .	30

# List of Tables

3.1	Initial electrical and mechanical system parameters . . . . .	16
3.2	Parameters of sphere magnets . . . . .	18
3.3	Coil parameters of different AWG . . . . .	20

# Acknowledgements

Throughout the writing of this thesis, I have received a great deal of support and assistance.

I would first like to thank my supervisor, Professor Brian Mann, whose expertise was invaluable in formulating the research questions and methodology. Your insightful feedback pushed me to sharpen my thinking and brought my work to a higher level.

I would like to acknowledge Angus Bowers. I want to thank you for your patient support to help me with my communication skills.

I would like to thank my family for their wise counsel and sympathetic ear. You are always there for me. Finally, I would like to thank my friend Rui Kang, who makes the tough 2020 less dull.

# Chapter 1

## Introduction

Electricity is essential in our lives and almost everything from mobile phones to medical devices needs constant power to keep them running. Keeping such devices plugged in or replacing batteries is inefficient, and used batteries can cause pollution. Therefore, it is desirable to have a compact generator that can provide electricity by excitation at low frequencies and low amplitudes, such as human motions. In this thesis, a spherical, rolling magnet generator for passive energy harvesting is investigated. It was designed for gathering energy from human motion.

While previous works mostly focus on generators driven by single dimension excitation. Bowers's paper investigated a similar device but focused entirely experiments on how the device performed under various input conditions. However, his work lacks the dynamic analysis of that device.[1] [2] [3] [4]

This thesis focuses on the dynamic analysis of this device and gives its governing equations. Under two expected applications, this thesis uses different numerical simulation parameters, finds the parameters that greatly influence its efficiency, and provides optimal parameter combinations.

The rest of the thesis is organized as follows: Chapter 2 describes a rolling sphere system's physical model and derives the equations of motion using Lagrange's equa-

tion. Chapter 3 investigates the numerical analysis of the rolling sphere under horizontal harmonic excitation and vertical harmonic excitation.

# Chapter 2

## Equation of Motion Derivation

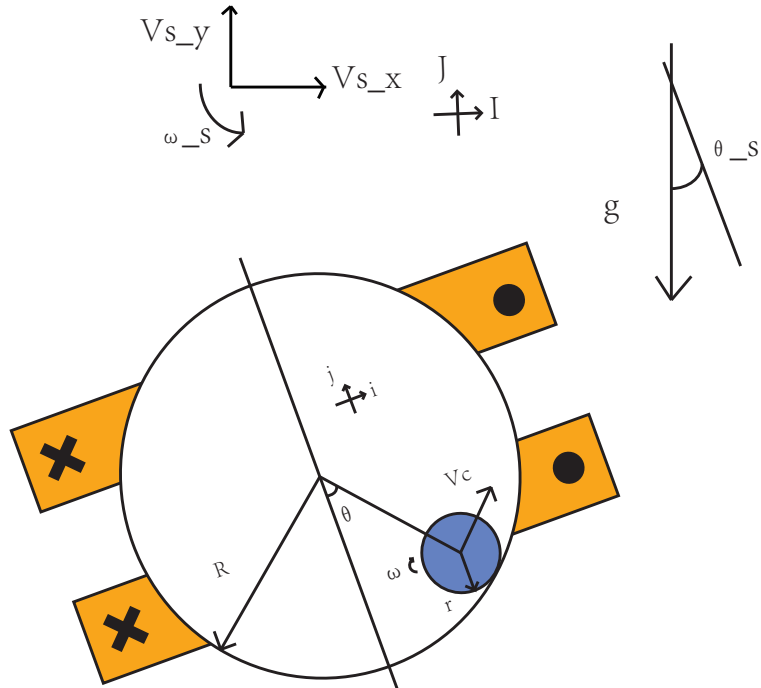


Figure 2.1: Schematic of sphere

Fig 2.1 shows a picture of the whole device, which is a big hollow sphere with a coil around it. A sphere magnet rolls inside the sphere without slip and does not lose contact with the sphere. We assume that the device only moves in 2D. We use Lagrange's equations to derive the equations of motion:

$$\frac{d}{dt} \left( \frac{\partial \mathcal{L}}{\partial \dot{q}_i} \right) - \frac{\partial \mathcal{L}}{\partial q_i} = Q_{q_i} \quad (2.1)$$

## 2.1 Mechanical equations

The hollow sphere was presumed to be moving in both the x-direction and y-direction and rotating in the x-y plane.

$$X_s = X_s(t) \quad (2.2)$$

$$Y_s = Y_s(t) \quad (2.3)$$

$$\theta_s = \theta_s(t) \quad (2.4)$$

$$\vec{v}_s = \dot{\vec{r}}_s = \dot{X}_s(t)\hat{I} + \dot{Y}_s(t)\hat{J} \quad (2.5)$$

$$\vec{\omega}_s = \dot{\theta}_s(t)\hat{K} \quad (2.6)$$

### 2.1.1 Lagrange equation in non-inertial system

We choose the hollow sphere as the reference frame, and it is a non-inertial system with acceleration  $a_s$  and angular velocity  $\omega_s$  :

$$a_s = \ddot{X}_s(t)\hat{I} + \ddot{Y}_s(t)\hat{J} \quad (2.7)$$

$$\vec{\omega}_s = \dot{\theta}_s(t)\hat{K} \quad (2.8)$$

In this non-inertial system, Lagrange equation has form [5]:

$$\frac{d}{dt} \left( \frac{\partial \mathcal{L}}{\partial \dot{q}_i} \right) - \frac{\partial \mathcal{L}}{\partial q_i} = Q_{q_i} + Q_{q_i r} \quad (2.9)$$

$$Q_{q_i r} = \Sigma(\vec{F}_{ei} + \vec{F}_{ci}) \cdot \frac{\partial \vec{r}_i}{\partial q_i} \quad (2.10)$$

Where  $Q_{q_i r}$  is non-inertial generalized force that appears in the  $i$ th equation,  $\vec{F}_{ei}$  is the force of transport and  $\vec{F}_{ci}$  is the Coriolis force.

$$\vec{F}_{ei} = -m[\vec{a}_s + \frac{d\vec{\omega}_s}{dt} \times \vec{r}_i + \vec{\omega}_s \times (\vec{\omega}_s \times \vec{r}_i)] \quad (2.11)$$

$$\vec{F}_{ci} = 2m(\vec{\omega}_s \times \dot{\vec{r}}_i) \quad (2.12)$$

### 2.1.2 Motion of the sphere magnet

The sphere magnet is a solid sphere of constant density. So the moments of inertia about an axis through its center of mass is:

$$I_c = \frac{2}{5}mr^2 \quad (2.13)$$

The sphere magnet has velocity:

$$\dot{\vec{r}}_c = \dot{x}\hat{i} + \dot{y}\hat{j} = v_c \cos(\theta)\hat{i} + v_c \sin(\theta)\hat{j} \quad (2.14)$$

$$v_c = \dot{\theta}(R - r) \quad (2.15)$$

The sphere magnet roll without slip:

$$v_c = \omega r \quad (2.16)$$

Now, we can calculate the kinetic energy  $\mathcal{T}$  and potential energy  $\mathcal{U}$  of the system.

The kinetic energy  $\mathcal{T}$  has two parts, mechanical kinetic energy  $\mathcal{T}_m$  and electrical kinetic energy  $\mathcal{T}_e$  which is discussed in section 2.2.

$$\mathcal{U} = mgy = -mg(R - r)\cos(\theta + \theta_s) \quad (2.17)$$

$$\mathcal{T}_m = \frac{1}{2}m\vec{v}_c \cdot \vec{v}_c + \frac{1}{2}I_c\omega^2 = \frac{7}{10}m\dot{\theta}^2(R - r)^2 \quad (2.18)$$

$Q_\theta$  is determined by inertial force  $\vec{F}$

$$\vec{F} = \vec{F}_{ei} + \vec{F}_{ci} = -m[\vec{a}_s + \frac{d\vec{\omega}_s}{dt} \times \vec{r}_i + \vec{\omega}_s \times (\vec{\omega}_s \times \vec{r}_i) - 2\vec{\omega}_s \times \dot{\vec{r}}_i] \quad (2.19)$$

$$Q_\theta = \vec{F} \cdot \frac{\partial \vec{r}}{\partial \theta} \quad (2.20)$$

## 2.2 Electrical equations

Fig 2.2 shows the electrical system circuit configuration diagram.  $R_L$  is the resistance of an external load,  $R_i$  is the internal resistance of the coil,  $L$  is the inductance of the coil, and  $V$  is the voltage across the coil.

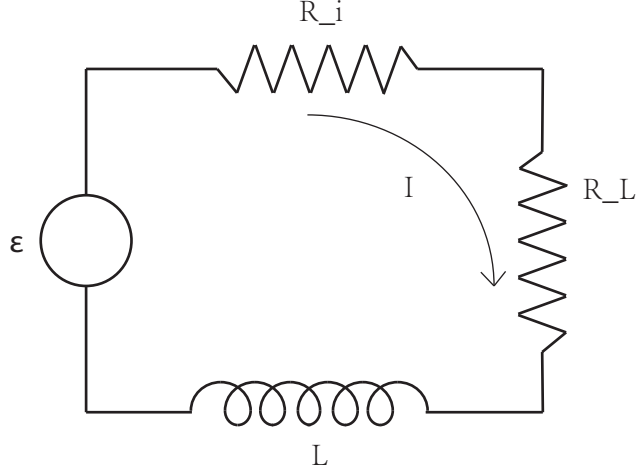


**Figure 2.2:** Electrical system circuit configuration diagram

### 2.2.1 Generalized Lagrange equation

In order to derive governing equations in this mechanical and electrical system, we need to use generalized Lagrange equation [6]:

$$\frac{d}{dt} \left( \frac{\partial \mathcal{T}}{\partial \dot{q}_i} \right) - \frac{\partial \mathcal{T}}{\partial q_i} + \frac{\partial \mathcal{D}}{\partial \dot{q}_i} + \frac{\partial \mathcal{U}}{\partial q_i} = Q_{q_i} + Q_{q_i r} \quad (2.21)$$

$$\mathcal{T} = \mathcal{T}_m + \mathcal{T}_e \quad (2.22)$$

$$\mathcal{T}_e = \frac{1}{2} L \dot{q}^2 + \mathcal{T}_c \quad (2.23)$$

Where  $L$  is the coil inductance,  $q$  is the charge coordinate and  $\mathcal{T}_c$  is the electromagnetic coupling energy term caused by magnet-coil interactions.  $\mathcal{D}$  is the non-

conservative term and is defined as:

$$\mathcal{D} = \frac{1}{2}(R_L + R_i)\dot{q}^2 \quad (2.24)$$

### 2.2.2 Magnet–coil interactions

In this subsection, we need to find electromagnetic coupling energy term  $\mathcal{T}_c$ . First, the magnetic fields  $\vec{B}$  of the sphere magnet will be modeled by a magnetic dipole. A magnetic dipole is a mathematical simplification of a magnet with a magnetic moment contained in an infinitesimal volume. The magnetic field  $\vec{B}$  generated by a dipole can be given by [3]:

$$\vec{B} = -\frac{\mu_0}{4\pi}\nabla\frac{\vec{m}_s \cdot \vec{r}_m}{|\vec{r}_m|^3} = -\frac{\mu_0}{4\pi}\left(\frac{\vec{m}_s}{|\vec{r}_m|^3} - (\vec{m}_s \cdot \vec{r}_m)\frac{3\vec{r}_m}{|\vec{r}_m|^5}\right) \quad (2.25)$$

Where  $\mu_0 = 4\pi \times 10^{-7}H/m$  is the permeability of free space, or magnetic constant,  $\nabla$  represents a vector gradient operation,  $\vec{m}_s$  is the magnetic moment of the dipole magnet,  $B_r$  is surface field and  $v_s$  is the volume of magnet.  $\vec{r}_m = \vec{r}_p - \vec{r}_s$  is a vector from the magnetic dipole to a given point.[9] The coordinate frame shows in Fig 2.3.

$$\vec{m}_s = \frac{B_r v_s}{\mu_0}(\sin\alpha, 0, \cos\alpha) \quad (2.26)$$

$$\vec{r}_p = (r_i \cos(\phi), r_i \sin(\phi), h) \quad (2.27)$$

$$\vec{r}_s = ((R - r) \sin\theta, 0, -(R - r)\cos\theta) \quad (2.28)$$

$$\vec{r}_m = \vec{r}_p - \vec{r}_s \quad (2.29)$$

$$B_z = \vec{B} \cdot \vec{z} \quad (2.30)$$

We assume the sphere magnet's initial position is the bottom of the hollow sphere,

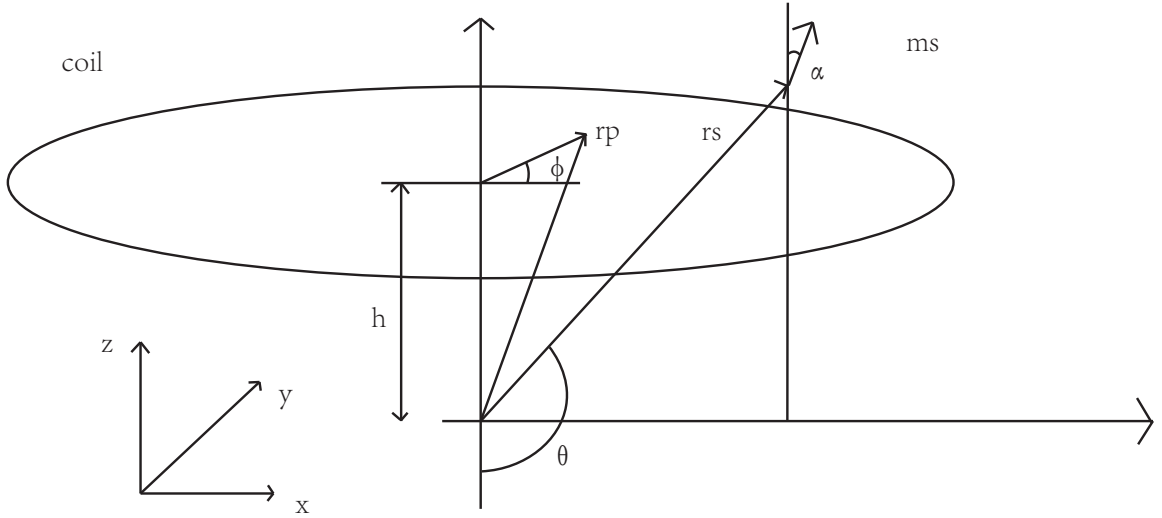


**Figure 2.3:** Schematic of magnet–coil interactions

and the dipole point to the hollow sphere's center. As shown in Fig 2.4, when the sphere magnet is rolling, the angle between the initial dipole direction and current dipole direction  $\alpha$  is given by

$$R\theta = r\alpha \quad (2.31)$$

In order to get the voltage resulting from electromagnetic interactions, we need to find the expression for the magnetic flux. Fig 2.3 shows the schematic to calculate the magnetic flux of a single-coil at height  $h$  from the center of the hollow sphere.

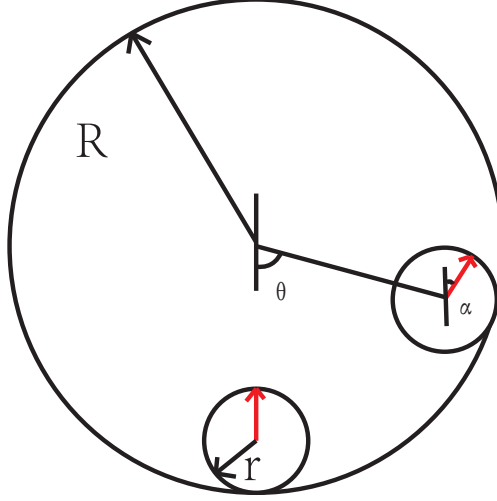


**Figure 2.4:** Dipole Direction

Fig 2.5 shows the whole coil. While in this situation,  $D$  minus  $d$  is quite small, so we consider  $D \approx d = 2 r_{coil}$ .  $\Phi$  is the magnetic flux of a single-coil, and  $\Phi_t$  is the total magnetic flux.

$$\Phi = \int_0^{2\pi} \int_0^{r_{coil}} B_z \cdot (r_i dr_i d\phi) \quad (2.32)$$

$$\Phi_t = \int_{-\frac{1}{2}H_c}^{\frac{1}{2}H_c} \Phi \frac{N_c}{H_c} dh \quad (2.33)$$

With the expression of the total magnet flux, Faraday's law is used to get the voltage across the coil. [10] When evaluating the time derivative, we find that only  $\theta$  will vary in time for this system. Therefore, with substitution, the voltage can be represented by:

$$\epsilon = -\frac{d\Phi_t}{dt} = f(\theta)\dot{\theta} \quad (2.34)$$

$$f(\theta) = -\frac{N_c}{H_c} \int_{-\frac{1}{2}H_c}^{\frac{1}{2}H_c} \int_0^{2\pi} \int_0^{r_{coil}} \frac{\partial B_z}{\partial \theta} \cdot (r_i dr_i d\phi dh) \quad (2.35)$$

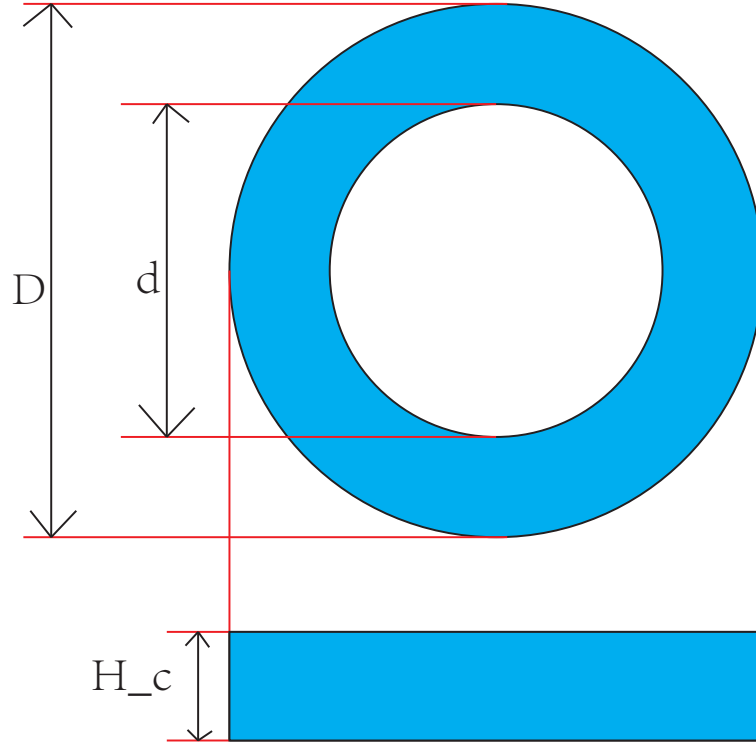


**Figure 2.5:** Coil size

In order to get the coupling energy term  $\mathcal{T}_c$ , we assume that the coil interactions result in very small energy losses from eddy currents and other effects, so the electrical and mechanical coupling energy are equal. Eddy current losses can not be ignored only for higher frequency cases or larger wire diameters than those used in this thesis.[7] [8]

$$\mathcal{T}_c = \int_0^t \epsilon \dot{q} dt = \int_0^t f(\theta) \dot{\theta} \dot{q} dt = \dot{q} \int_0^\theta f(\theta) d\theta \quad (2.36)$$

## 2.3 Governing equations

Applying  $\mathcal{T}$ ,  $\mathcal{D}$  and  $\mathcal{U}$  into the generalized Lagrange equation.

$$\frac{d}{dt} \left( \frac{\partial \mathcal{T}}{\partial \dot{q}_i} \right) - \frac{\partial \mathcal{T}}{\partial q_i} + \frac{\partial \mathcal{D}}{\partial \dot{q}_i} + \frac{\partial \mathcal{U}}{\partial q_i} = Q_{q_i} + Q_{q_i r} \quad (2.37)$$

$$\mathcal{T} = \mathcal{T}_m + \mathcal{T}_e \quad (2.38)$$

$$\mathcal{T}_m = \frac{7}{10} m \dot{\theta}^2 (R - r)^2 \quad (2.39)$$

$$\mathcal{T}_e = \frac{1}{2} L \dot{q}^2 + \mathcal{T}_c \quad (2.40)$$

$$\mathcal{D} = \frac{1}{2} (R_L + R_i) \dot{q}^2 \quad (2.41)$$

$$\mathcal{T}_c = \dot{q} \int_0^\theta f(\theta) d\theta \quad (2.42)$$

Using  $\theta$  as the generalized coordinate to get the mechanical equation.

$$\begin{aligned} & \frac{7}{5} m \ddot{\theta} (R - r)^2 + mg(R - r) \sin(\theta + \theta_s) - f(\theta) \dot{q} \\ & = -m(R - r) [\ddot{X}_s(t) \cos(\theta + \theta_s) + \ddot{Y}_s(t) \sin(\theta + \theta_s) + \dot{\omega}_s (R - r)] \end{aligned} \quad (2.43)$$

Then, choose  $q$  as generalized coordinate to get the electrical differential equation.

$$L \ddot{q} + \dot{q} (R_L + R_i) + f(\theta) \dot{\theta} = 0 \quad (2.44)$$

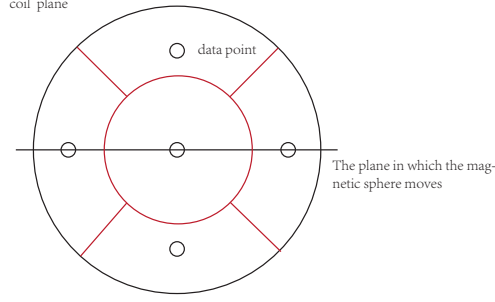


**Figure 2.6:** Data points in the coil plane

### 2.3.1 Simplification of $f(\theta)$

In this subsection, we need to find  $f(\theta)$  which is defined by:

$$f(\theta) == -\frac{N_c}{H_c} \int_{-\frac{1}{2}H_c}^{\frac{1}{2}H_c} \int_0^{2\pi} \int_0^{r_{coil}} \frac{\partial B_z}{\partial \theta} \cdot (r_i dr_i d\phi dh) \quad (2.45)$$

It is inefficient to calculate the exact expression of  $f(\theta)$ , so we solve for an approximation of  $f(\theta)$ . For the magnet flux of a single-coil, choose 5 points (shown in Fig 2.6) in the coil plane and calculate  $\frac{\partial B_z}{\partial \theta}$  in these points. Then take the average of them and times the coil area, then integrate over height to get the total flux.

$$f(\theta) == -\frac{N_c}{H_c} \int_{-\frac{1}{2}H_c}^{\frac{1}{2}H_c} \frac{\partial \bar{B}_z}{\partial \theta} \pi r_{coil}^2 dh \quad (2.46)$$

$$\vec{r}_{pj} = (r_j \cos(\phi), r_j \sin(\phi), h) \quad (j = 1 \ 5) \quad (2.47)$$

$$\vec{r}_s = ((R - r) \cos(\theta - \frac{\pi}{2}), 0, (R - r) \sin(\theta - \frac{\pi}{2})) \quad (2.48)$$

$$\vec{r}_{mj} = \vec{r}_{pj} - \vec{r}_s \quad (2.49)$$

$$\bar{B}_z = -\frac{\mu_0}{20\pi} \sum_{j=1}^5 \nabla \frac{\vec{m}_s \cdot \vec{r}_{mj}}{|\vec{r}_{mj}|^3} \quad (2.50)$$

# Chapter 3

## Numerical Simulation

This Chapter investigates applying harmonic excitation on the hollow sphere and uses command `ode45` in Matlab to find the numerical solutions to the governing equations. Then we change parameters to observe the change in efficiency, compare the data obtained, and give comments on the performance of the device under different sphere magnets and wires of the coil. At the end of each section, optimal parameter combinations for each expected application are provided. Table 3.1 shows initial electrical and mechanical system parameters. Fig 3.1 shows value of  $f(\theta)$  from 0 to  $2\pi$  under initial system parameters.

### 3.1 Horizontal harmonic excitation

In this section, horizontal harmonic excitation is applying on the hollow sphere.

$$X_s = X_s(t) = A \sin(\omega_0 t) \quad (3.1)$$

$$Y_s = 0 \quad (3.2)$$

$$\theta_s = 0 \quad (3.3)$$

**Table 3.1:** Initial electrical and mechanical system parameters

Parameter	Value	Units
AWG of coil	34	-
Type of sphere magnet	s7	-
Coil inductance, L	357	mH
Number of coil turns, $N_c$	2329	-
Coil inner circle diameter, d	6.0	cm
Coil outer circle diameter, D	6.5	cm
Height of coil, $H_c$	3.0	cm
Hollow sphere radius, R	2.5	cm
Sphere magnet radius, r	0.5	cm
Sphere magnet mass, m	5.4	g
External load resistance, $R_L$	300	$\Omega$
Sphere magnet surface field, $B_r$	0.8815	T
Excitation amplitude, A	0.5	m
Excitation frequency, $\omega$	$4\pi$	rad/s

$$\vec{v}_s = \dot{\vec{r}}_s = \dot{X}_s(t)\hat{I} = A\omega_0 \cos(\omega_0 t)\hat{I} \quad (3.4)$$

Where A is the amplitude and  $\omega_0$  is the angular frequency of the harmonic excitation.

From chapter 2, we have governing equations:

$$\frac{7}{5}m\ddot{\theta}(R-r)^2 + mg(R-r)\sin(\theta) - f(\theta)\dot{q} = mA\omega_0^2(R-r)\sin(\omega_0 t)\cos(\theta) \quad (3.5)$$

$$L\ddot{q} + \dot{q}(R_L + R_i) + f(\theta)\dot{\theta} = 0 \quad (3.6)$$

### 3.1.1 Different sphere magnet

This subsection focus on different sphere magnets. Note that different types of sphere magnets mean different sizes, mass and magnetic moment. When the radius is large, the volume is also large, cause the magnetic moment becomes large, which is good

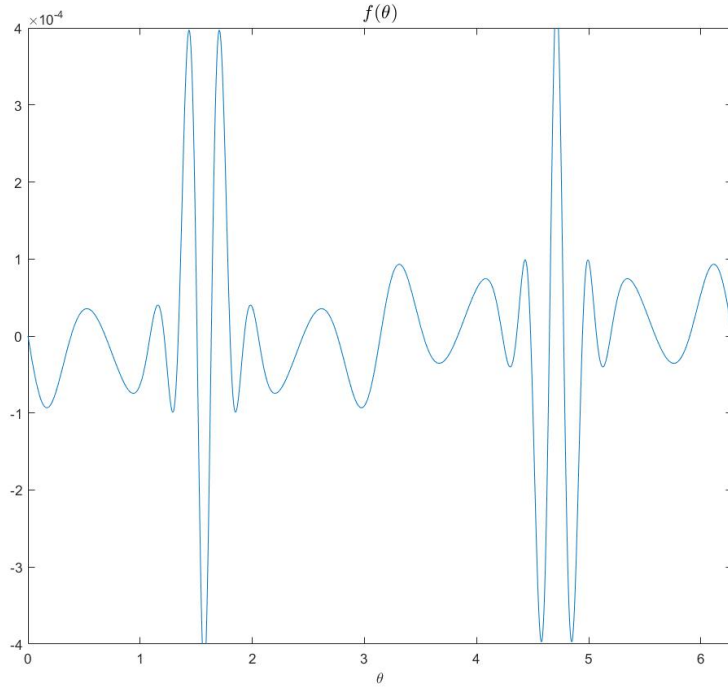


**Figure 3.1:**  $f(\theta)$  under initial parameters

for generating larger voltage. On the other hand, a large radius causes a large mass, which means the sphere magnet is harder to drive by the excitation. Besides, the radius of the magnet has a huge influence on  $f(\theta)$ , which is the key function of governing equations. So, it is difficult to judge which magnet is better. Table 3.2 shows the mass  $m$ , radius  $r$ , and surface field  $B_r$  of each magnet used in this section. [11] Fig 3.3 shows instantaneous power of each sphere magnet. Fig 3.4 shows the mean power and RMS voltage of each magnet. From fig 3.4, we find that when the radius is small, the mean power and RMS voltage increases with the radius. They reach a peak at  $sA$ . The max mean power is  $0.0341W$ , and the max RMS voltage is  $3.1992V$ .

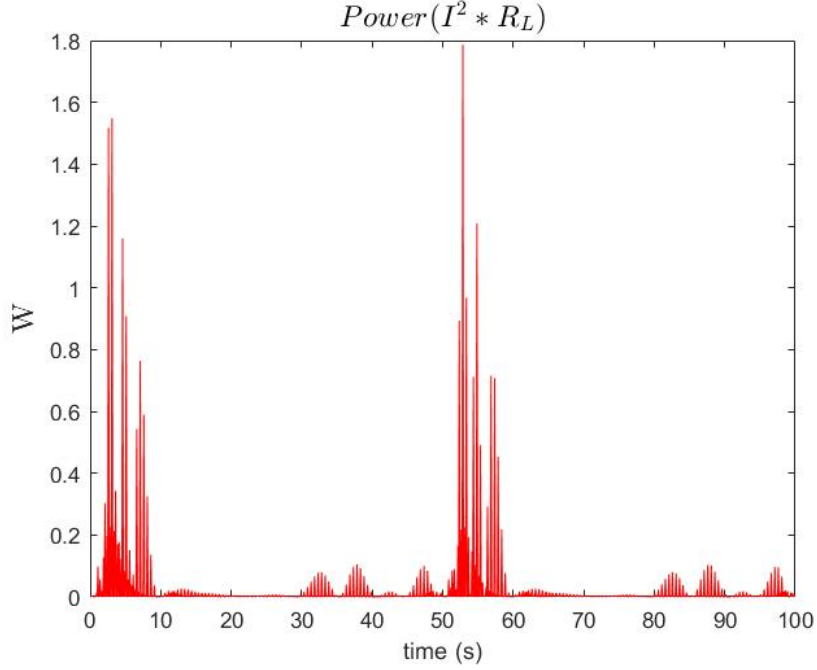


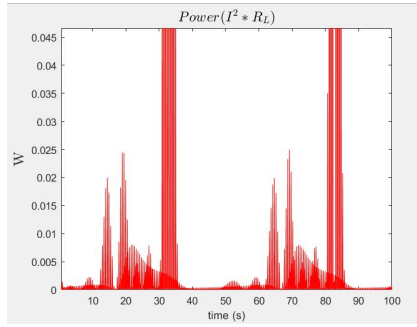
**Figure 3.2:** Instantaneous power under initial parameters

**Table 3.2:** Parameters of sphere magnets

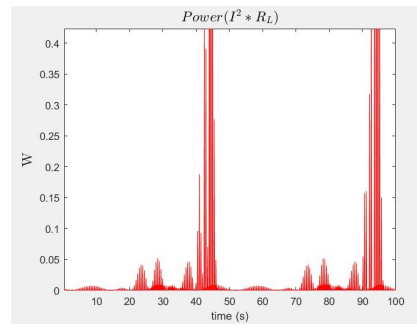
Type	r(cm)	m(g)	$B_r$ (T)
s5	0.40	2.0	0.8815
s6	0.45	3.4	0.8815
s7	0.50	5.4	0.8815
sA	0.80	15.7	0.8815
sC	0.95	27.2	0.8815

### 3.1.2 Different AWG

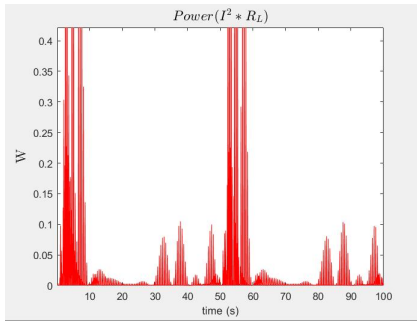
This subsection focus on the wire and coil. The inductance and resistance will change if the number of turns or AWG, a standardized wire gauge system called American Wire Gauge, of coil changes. [13] This section shows a comparison of different AWG with the same coil size. When the coil's size is determined, a large AWG, which means small wire diameter, will cause large inductance and number of turns, which is good



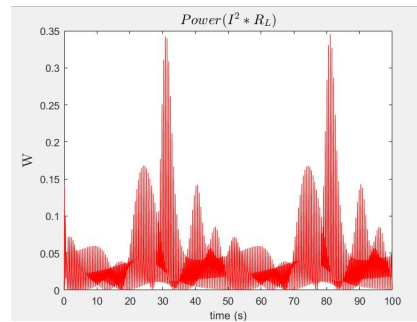
(a) s5



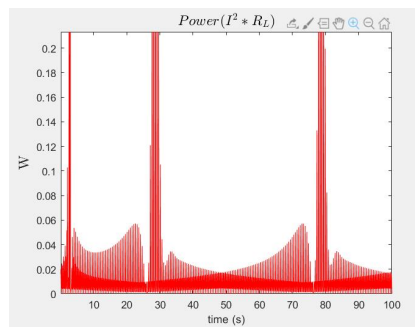
(b) s6



(c) s7



(d) sA



(e) sC

**Figure 3.3:** Instantaneous power of each sphere magnet

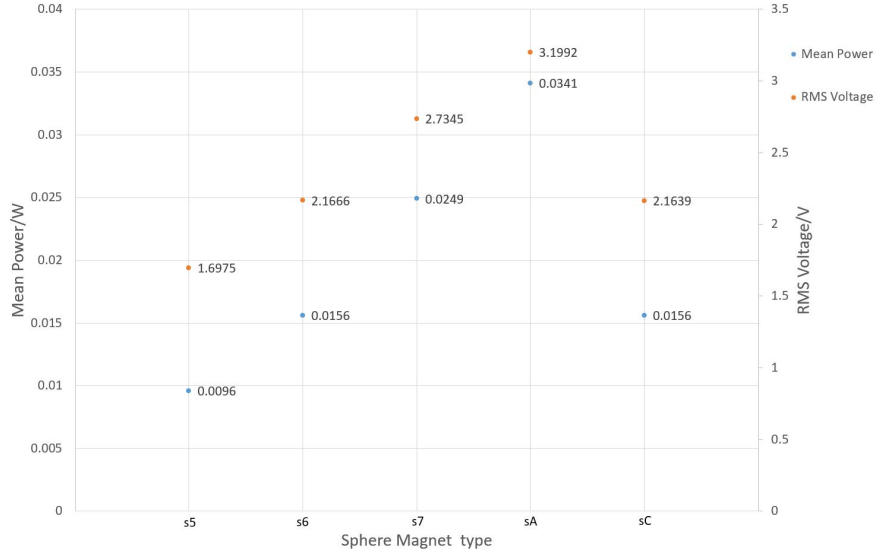
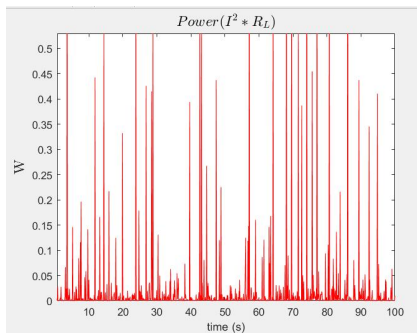


**Figure 3.4:** Mean Power and RMS Voltage of each magnet

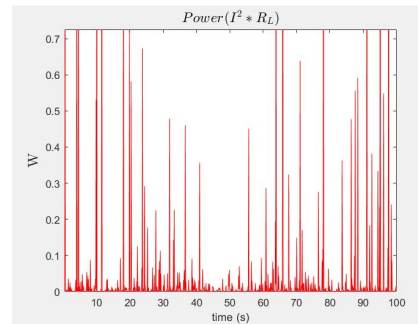
**Table 3.3:** Coil parameters of different AWG

AWG	L(mH)	$R_i(\Omega)$	N	d(cm)	D(cm)	$H_c$ (cm)
29	38	39	763	6.0	6.5	3.0
30	62	64	973	6.0	6.5	3.0
31	95	101	1204	6.0	6.5	3.0
32	143	153	1477	6.0	6.5	3.0
33	211	236	1794	6.0	6.5	3.0
34	357	391	2329	6.0	6.5	3.0
35	519	596	2812	6.0	6.5	3.0
36	816	938	3522	6.0	6.5	3.0

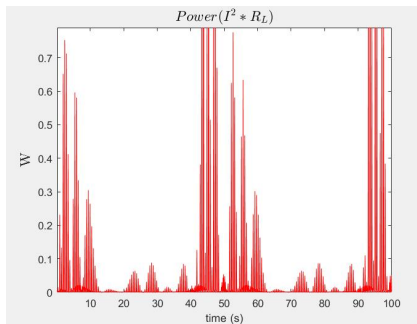
for generating larger voltage. On the contrary, large AWG will cause large resistance since the length of the wire increases, and the diameter of the wire is decreases. Table 3.3 shows parameters of each AWG. [12] Fig 3.5 and 3.6 shows instantaneous power of AWG 29 to 36. Fig 3.7 shows the mean power and RMS voltage of each AWG. From fig 3.7 shows that when the AWG is small, the mean power and RMS voltage increases with the AWG. They reach a peak at AWG 31, it slowly decreases. The max mean power is 0.0380W, and the max RMS voltage is 3.377V.



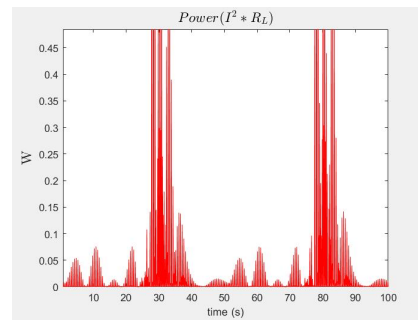
(a) AWG 29



(b) AWG 30

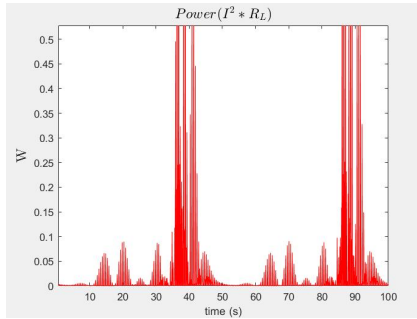


(c) AWG 31

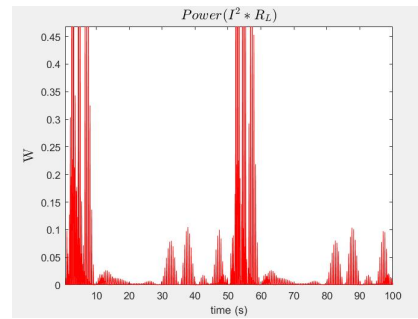


(d) AWG 32

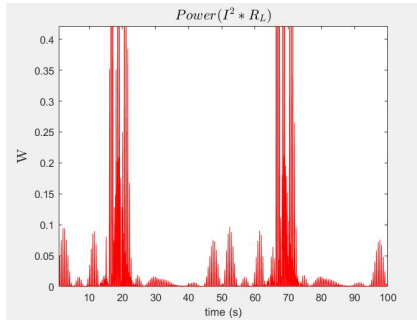
**Figure 3.5:** Instantaneous power from AWG 29 to 32



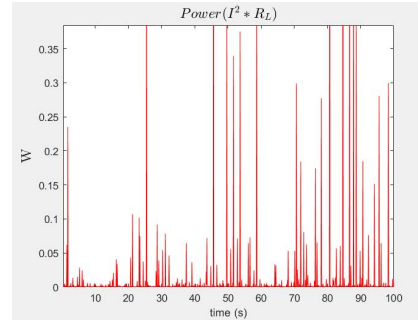
(a) AWG 33



(b) AWG 34



(c) AWG 35



(d) AWG 36

**Figure 3.6:** Instantaneous power from AWG 33 to 36

### 3.1.3 Optimal parameter combination

From subsection 3.1.1 and 3.1.2, we find that the best sphere magnet is sA and the best AWG is 31. Fig 3.8 shows instantaneous power and fig 3.9 shows instantaneous voltage under this parameters. The mean power is 0.0678W, and the RMS voltage is 4.5116V

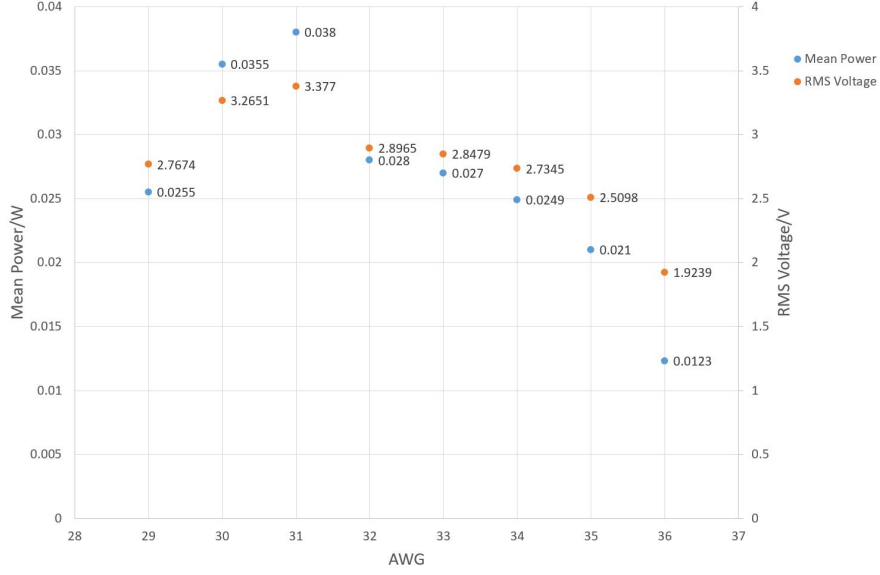


Figure 3.7: Mean Power and RMS Voltage of each AWG

## 3.2 Vertical harmonic excitation

In this section, vertical harmonic excitation is applying on the hollow sphere, and the rest is the same as in section 3.1.

$$X_s = 0 \quad (3.7)$$

$$Y_s = Y_s(t) = A \sin(\omega_0 t) \quad (3.8)$$

$$\theta_s = 0 \quad (3.9)$$

$$\vec{v}_s = \dot{\vec{r}}_s = \dot{Y}_s(t) \hat{J} = A\omega_0 \cos(\omega_0 t) \hat{J} \quad (3.10)$$

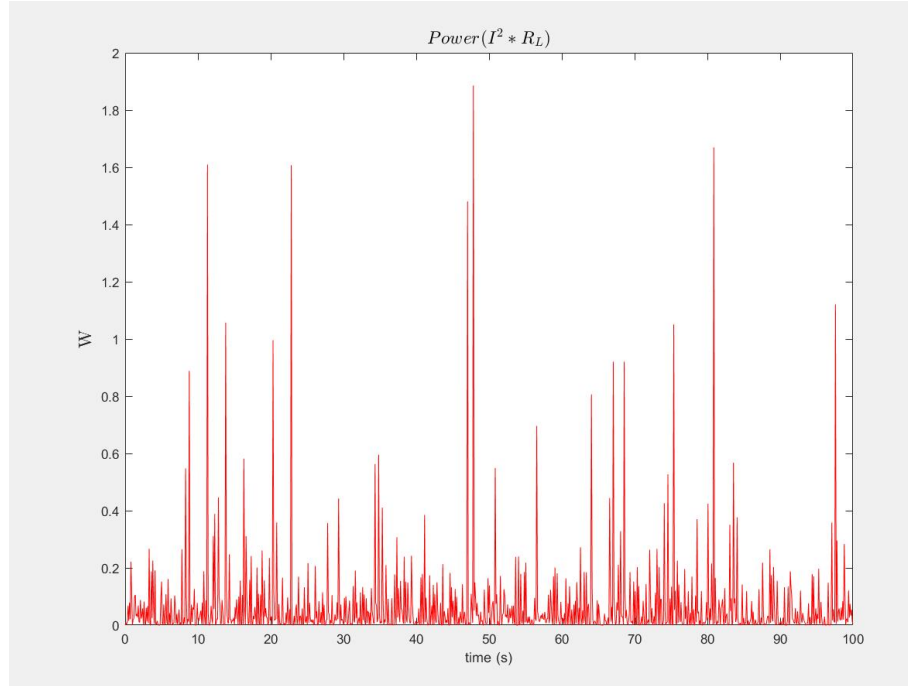


**Figure 3.8:** Instantaneous power

Where  $A$  is the amplitude and  $\omega_0$  is the angular frequency of the harmonic excitation.

From chapter 2, we have governing equations:

$$\frac{7}{5}m\ddot{\theta}(R-r)^2 + mg(R-r)\sin(\theta) - f(\theta)\dot{q} = mA\omega_0^2(R-r)\sin(\omega_0 t)\sin(\theta) \quad (3.11)$$

$$L\ddot{q} + \dot{q}(R_L + R_i) + f(\theta)\dot{\theta} = 0 \quad (3.12)$$

### 3.2.1 Different sphere magnet

Same as subsection 3.1.1, table 3.2 shows the mass  $m$ , radius  $r$ , and surface field  $B_r$  of each magnet used in this section. Fig 3.10 shows instantaneous power of each sphere magnet. Fig 3.11 shows the mean power and RMS voltage of each magnet. From

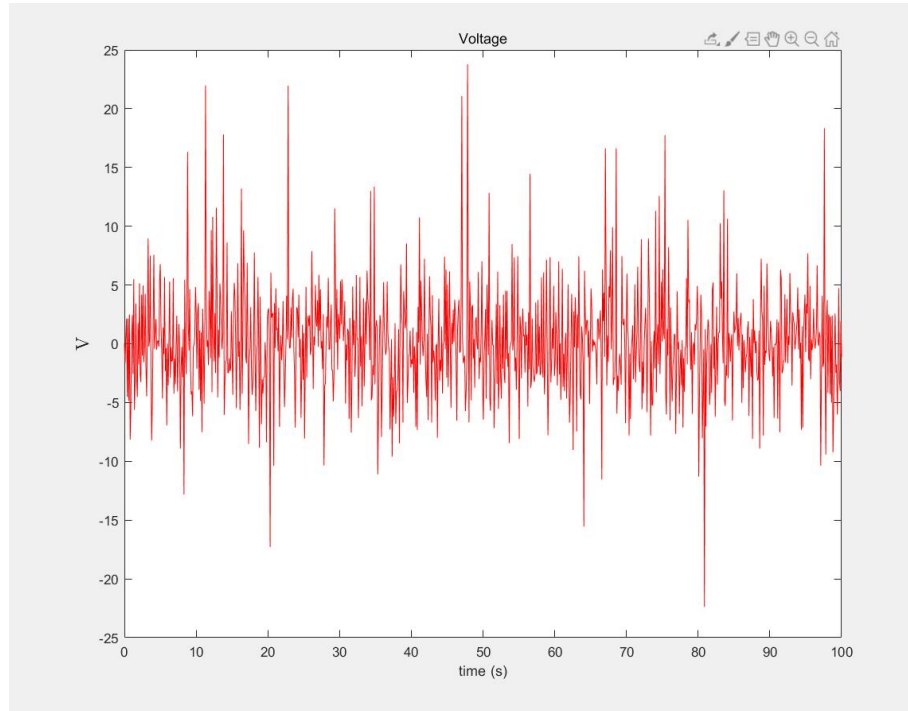
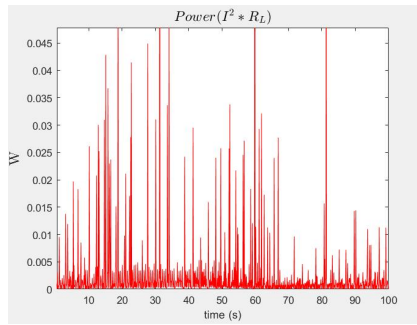


**Figure 3.9:** Instantaneous voltage

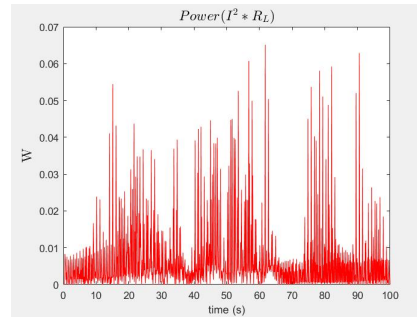
fig 3.11, we find that when the radius is small, the mean power and RMS voltage increases with the radius. They reach a peak at s7. Unlike horizontal excitation, mean power and RMS voltage decrease rapidly after the peak, and they are all small than data under horizontal excitation. The max mean power is 0.0098W, and the max RMS voltage is 1.7144V.

### 3.2.2 Different AWG

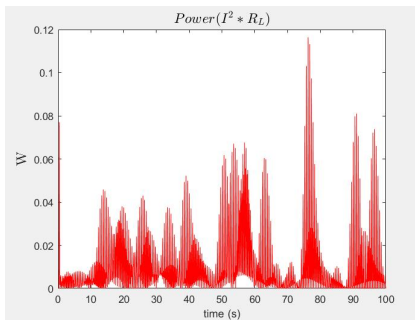
Same as subsection 3.1.2, table 3.3 shows parameters of each AWG. Fig 3.12 and 3.13 shows instantaneous power of AWG 29 to 36. Fig 3.14 shows the mean power and RMS voltage of each AWG. From fig 3.14, unlike the horizontal case, the mean power and RMS voltage are not monotonically increasing with the AWG before the



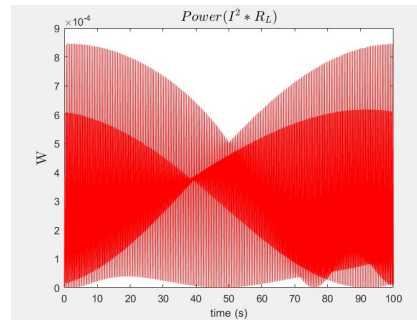
(a) s5



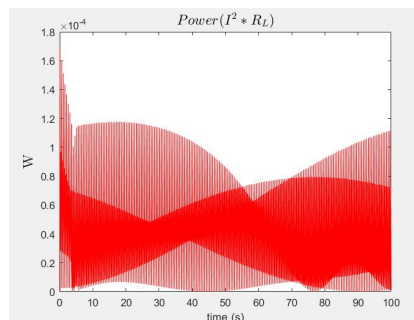
(b) s6



(c) s7



(d) sA



(e) sC

**Figure 3.10:** Instantaneous power of each sphere magnet

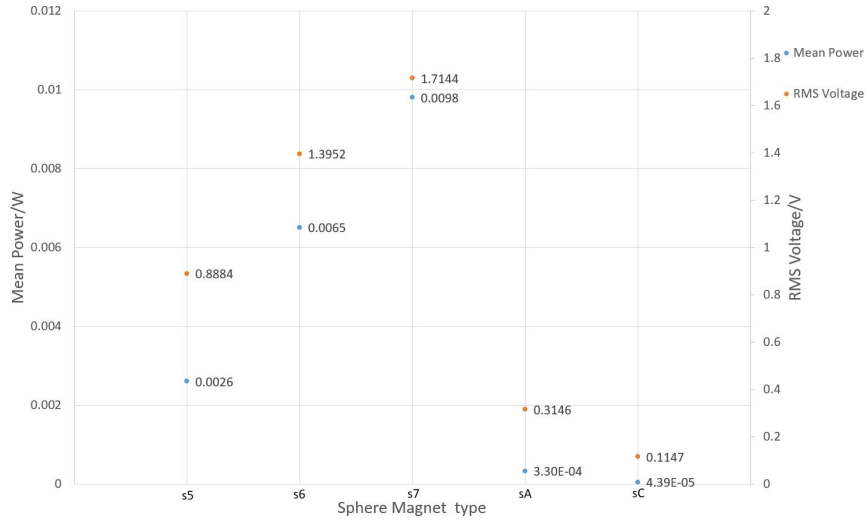
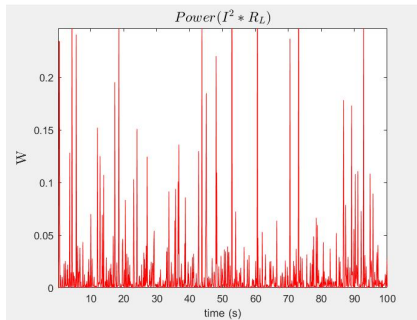


**Figure 3.11:** Mean Power and RMS Voltage of each magnet

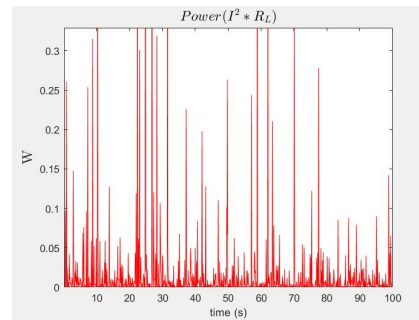
peak. It is fluctuating around AWG 31. Same with the horizontal case, the mean power and RMS voltage slowly decrease after they reach the peak. The max mean power is 0.0186W, and the max RMS voltage is 2.3609V.

### 3.2.3 Optimal parameter combination

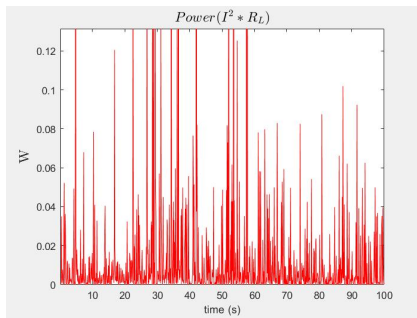
From subsection 3.2.1 and 3.2.2, we find that the best sphere magnet is s7 and the best AWG is 32. Fig 3.15 shows instantaneous power and fig 3.16 shows instantaneous voltage under this parameters. The mean power is 0.0186W, and the RMS voltage is 2.3609V



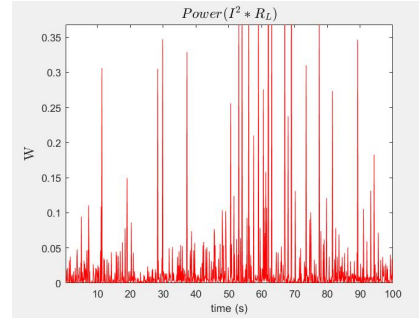
(a) AWG 29



(b) AWG 30

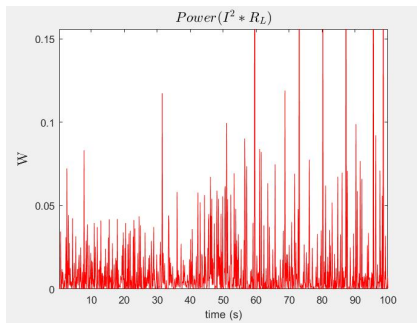


(c) AWG 31

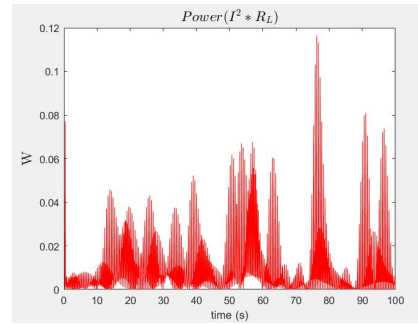


(d) AWG 32

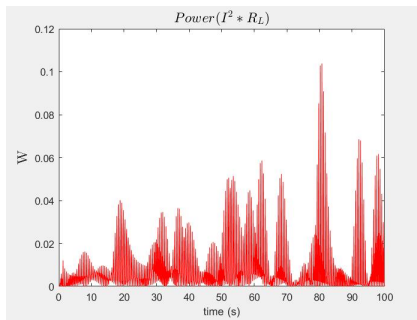
**Figure 3.12:** Instantaneous power from AWG 29 to 32



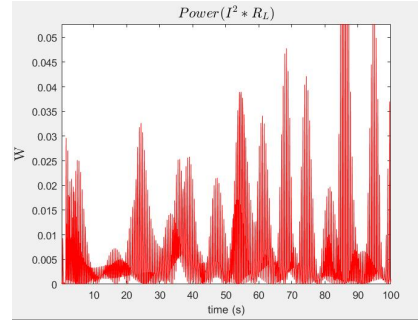
(a) AWG 33



(b) AWG 34



(c) AWG 35



(d) AWG 36

**Figure 3.13:** Instantaneous power from AWG 33 to 36

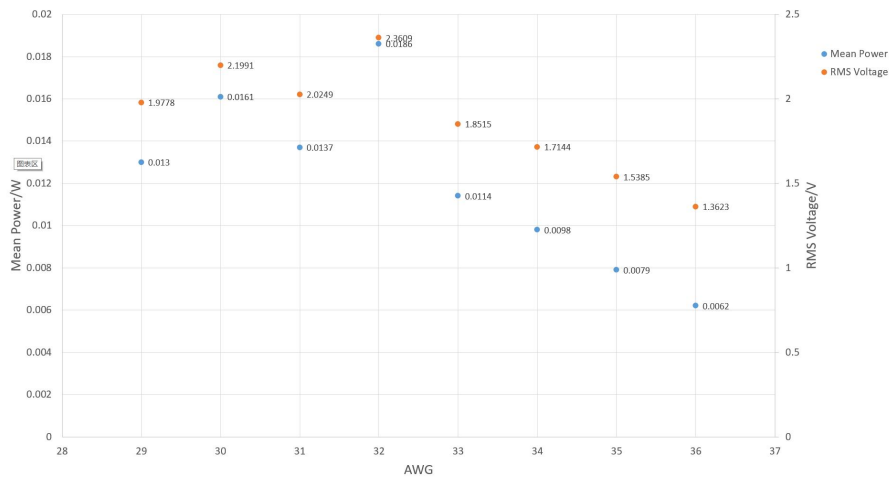


**Figure 3.14:** Mean Power and RMS Voltage of each AWG

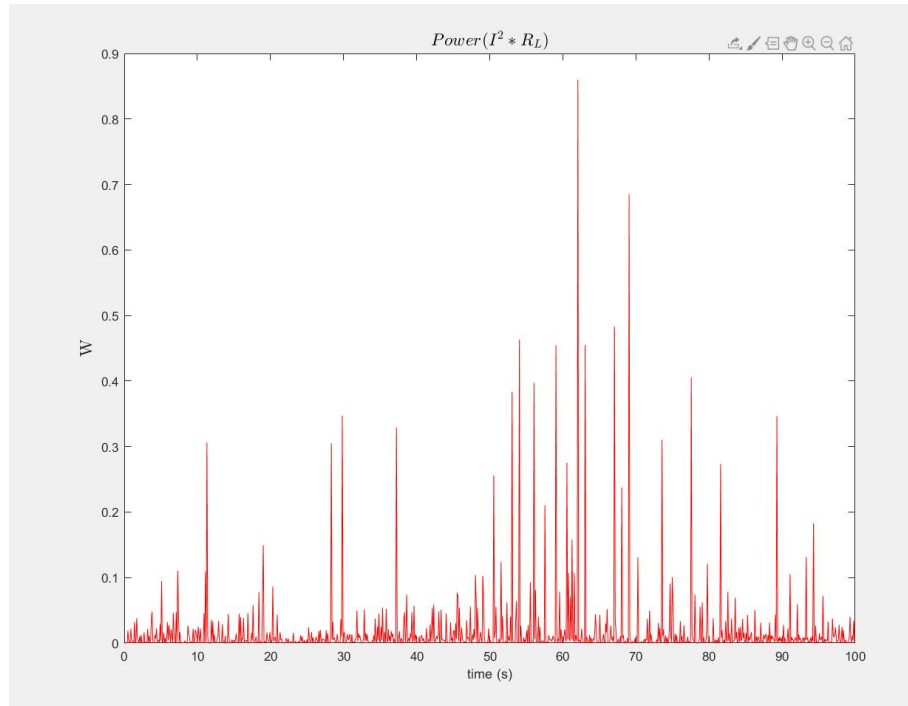


**Figure 3.15:** Instantaneous power

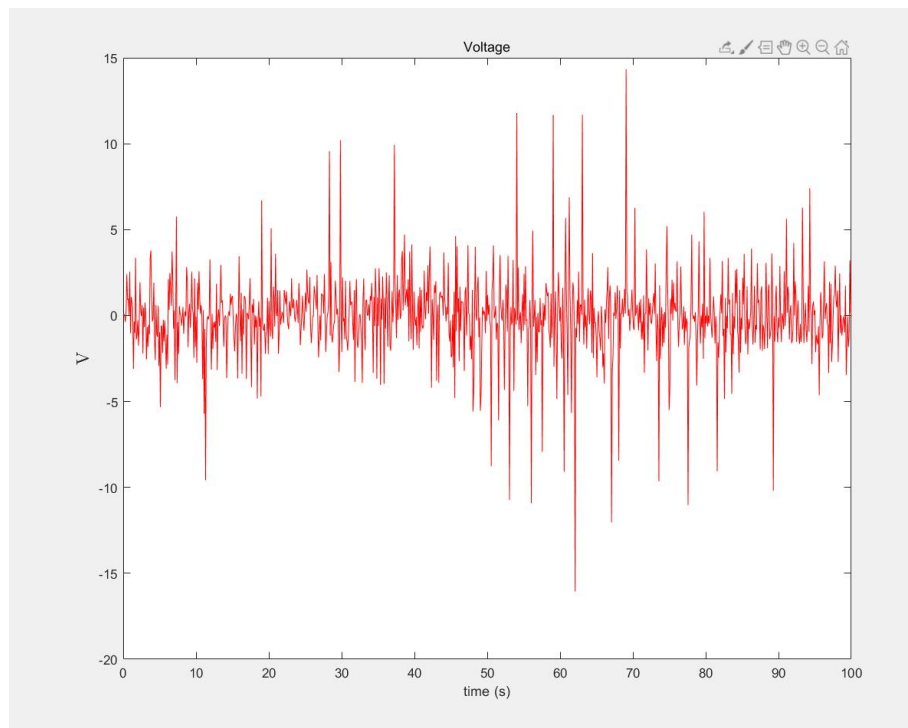


**Figure 3.16:** Instantaneous voltage

# Chapter 4

## Conclusions

In this thesis, a spherical, rolling magnet generator for passive energy harvesting was investigated. In the first part of this thesis, the governing equations were obtained using the generalized Lagrange equation in the non-inertial system. The second part used Matlab for numerical simulation to investigate the influence of different sphere magnets and AWG of coils on efficiency under two expected applications, horizontal harmonic excitation, and vertical harmonic excitation.

For the horizontal harmonic excitation case, the simulation was divided into two parts. In the first part, with five different sphere magnets and the same AWG of the coil, AWG 34, the mean power and RMS voltage were compared, and the data of sA has a maximum. In the second part, with the same sphere magnet, type s7, and different AWG of the coil, from AWG 29 to 36, the mean power and RMS voltage were compared, and the data of AWG 31 has a maximum.

For the vertical harmonic excitation case, the simulation is also divided into two parts. In the first part, with five different sphere magnets and the same AWG of the coil, AWG 34, the mean power and RMS voltage were compared, and the data of s7 has a maximum. In the second part, with the same sphere magnet, type s7, and different AWG of the coil, from AWG 29 to 36, the mean power and RMS voltage

were compared, and the data of AWG 32 has a maximum.

Also, with the same sphere magnet and AWG of the coil, horizontal case data were always bigger than vertical case data. So, we try to avoid using this device under vertical excitation.

## 4.1 Future work

This thesis focus on a 2D case in which the whole system moves only in two dimensions. While in the real world, the sphere magnet will move in all three dimensions. Besides, in this thesis, we assume the sphere magnet always contacts the hollow sphere. While in the real world, the sphere magnet may lose contact with the hollow sphere when its velocity is too small and strike the hollow sphere. When this happens, it will cause energy loss, and we cannot simply use Lagrange's equation as this thesis did. The next step is to build a 3D model and remove the assumption that the sphere magnet always contacts the hollow sphere.

## Bibliography

- [1] Vishwas Bedekar, Josiah Oliver, and Shashank Priya. Pen harvester for powering a pulse rate sensor. *Journal of Physics D: Applied Physics*, 42(10):105105, apr 2009.
- [2] B.P. Mann and B.A. Owens. Investigations of a nonlinear energy harvester with a bistable potential well. *Journal of Sound and Vibration*, 329(9):1215–1226, 2010.
- [3] B.P. Mann and N.D. Sims. Energy harvesting from the nonlinear oscillations of magnetic levitation. *Journal of Sound and Vibration*, 319(1):515–530, 2009.
- [4] Benjamin J Bowers and David P Arnold. Spherical, rolling magnet generators for passive energy harvesting from human motion. *Journal of Micromechanics and Microengineering*, 19(9):094008, aug 2009.
- [5] Stroe, Ion, and Andrei Craifaleanu. “Generalization of the Lagrange Equations Formalism, for Motions with Respect to Non-Inertial Reference Frames.” *Applied Mechanics and Materials*, vol. 656, Trans Tech Publications, Ltd., Oct. 2014, pp. 171–180. Crossref, doi:10.4028/www.scientific.net/amm.656.171.
- [6] A.Preumont, *Mechatronics: Dynamics of Electromechanical and Piezoelectric Systems*, Springer, Dordrecht, 2006.
- [7] A.J.Sneller, B.P.Mann, On the nonlinear electromagnetic coupling between a coil and an oscillating magnet, *Journal of Physics D: Applied Physics* 43 (29) (2010)295005.doi:10.1088/0022-3727/43/29/295005.
- [8] H.H.Woodson, J.R.Melcher, *Electromechanical Dynamics*, Wiley, New York, 1968.
- [9] K.W.Yung, P.B.Landecker, D.D.Villani, An analytic solution for the force between two magnetic dipoles, *Magnetic and Electrical Separation* 9 (1) (1998) 39–52.

- [10] J.V.Stewart, Intermediate Electromagnetic Theory, World Scientific,Singapore, River Edge,NJ,2001.
  
- [11] Sphere Magnets, K&J Magnetics, Inc. <https://www.kjmagnetics.com/>
  
- [12] Multi-layer coil inductance value calculator, International Knowledge Centre for Engineering Sciences and Technology, <http://drr.ikcest.org/app/s0056>
  
- [13] American wire gauge, [https://en.wikipedia.org/wiki/American\\_wire\\_gauge](https://en.wikipedia.org/wiki/American_wire_gauge)